Formulation for critical shear stress of cohesive sediment mixture

Umesh K. Singh[1],*, Z. Ahmad[1] and Ashish Kumar[2]

[1]Department of Civil Engineering, Indian Institute of Technology Roorkee, Roorkee 247 667, India
[2]Department of Civil Engineering, Jaypee University of Information Technology, Waknaghat, Solan 173 234, India

This article describes results of an experimental study on incipient motion of gravel particles present in the cohesive mixtures, i.e. clay–silt–gravel and clay–silt–sand–gravel, in which the percentage of clay varied from 10% to 50% on weight basis. Incipient motion condition is visually and quantitatively identified which responds to sheet and line erosion type appearance on the top surface of the channel bed for clay up to 30% and mass erosion pattern for 40% and 50% of clay. The clay percentage, weighted geometric standard deviation and bulk density of the cohesive sediment mixture are found to be the main parameters that affect the incipient motion of gravel particles. A functional relationship is proposed to determine critical shear stress of gravel particles present in cohesive sediment mixtures. The regression analyses as well as goodness of fit test were conducted for the proposed relationships which were found to be in good agreement with the present data.

UNDERSTANDING of incipient motion of sediment particles is needed for estimation of sediment transport. The incipient motion is characterized as the beginning of the movement of bed particle when the flow-induced shear stress over the bed exceeds to a certain critical value. Shields[1] has been a pioneer in introducing the incipient motion curve widely known as Shields curve for computation of critical shear stress of uniform cohesionless sediment. Subsequently, incipient motion for uniform cohesionless sediments was studied by various workers[2–4]. River bed material consists of a mixture of cohesive as well as cohesionless materials. Singh et al.[5] reported that the Ganga River bed consists of sediments having clay, silt, sand and gravel. In the Indian context numerical modelling studies have been conducted to understand the characteristics of suspended sediment concentration in the stretches of the estuarine environment for Hooghly River[6–8] and for commonly occurring sandy particles in coastal areas[9]. Incipient motion plays an instrumental role in addressing the sediment-related problems in the riverine system such as reservoir sedimentation, hydraulic

structure failures, aggradation and degradation, flood inundation, water quality, siltation, navigation, etc. Most studies on incipient motion for cohesive mixture are reported on a mixture of clay, silt and sand[10–12]. Kothyari and Jain[13] reported a study of incipient motion for cohesive mixtures of clay–gravel and clay–sand–gravel. To our knowledge, no study has yet been reported on the incipient motion of gravel particles in a cohesive mixture of clay–silt–gravel and clay–silt–sand–gravel. Visual observation method to identify incipient motion condition was adopted earlier by Kothyari and Jain[13]. However, in the present study quantitative measurement of sediment transport rate was also included for reinforcing the reliability of visual observations. The present study attempts to develop a relation for computation of critical shear stress of gravel particles in cohesive mixtures of clay–silt–gravel and clay–silt–sand–gravel. The computation of critical shear stress is well established for uniform cohesionless sediment. However, in case of non-uniform sediment the concept of unequal mobility of particles comes into consideration. The fraction-wise movement of particles in the non-uniform sediment mixture is known as unequal mobility of particles[14–17]. In the past, most investigators used the correction factor for computation of critical shear stress in case of non-uniform sediment. For example, Bridge and Bennett[18] used the correction factor as a function of individual particle size and arithmetic mean of non-uniform sediment. Patel and Ranga Raju[15] used a correction factor in terms of Kramer's uniformity coefficient which is a function of particle size and its percentage. Wu et al.[16] used hiding-exposure probability as a correction factor which is a function of particle size and its percentage. The present study uses a different form of correction factor that includes the same parameters as used by previous workers. Sutarto et al.[19] performed the stability analysis of semi-cohesive stream bank by considering the soil heterogeneity in the stream bank. In the present experimental study, the channel has mobile cohesive bed (not the bank), which is assumed to be homogeneous over the working section. The sidewall correction is needed in laboratory flumes on account of differences in surface roughness between channel bed and sidewalls (made of glass in the present study). Hence for computation of critical shear stress, the concept of effective shear stress on the channel bed was applied using

---

Manning–Strickler roughness coefficient according to Einstein[20] instead of total shear stress. This approach of sidewall correction was adopted in earlier studies[21–23].

In the present study, the expression proposed earlier[13,24] for estimation of critical shear stress has been used for analysis. Brownlie[24] proposed the following formula to compute the dimensionless critical shear stress for the cohesionless sediment which can be used in place of the Shields curve.

$$\tau_{*cm} = 0.22Y + 0.06(10)^{-7.7Y}, \tag{1}$$

where

$$Y = (\sqrt{(\rho_s - \rho)g(d)^3/\rho\nu^2})^{-0.6}.$$

τ_{*cm} is the dimensionless critical shear stress for the cohesionless sediment; ρ_s and ρ are the particle and fluid densities (kg/m^3) respectively; g the gravitational acceleration (m/s^2); d the arithmetic mean size of the cohesionless sediment (m); and ν the kinematic viscosity (m^2/s). Kothyari and Jain[13] studied the influence of cohesion on the incipient motion of cohesive sediment mixture of clay–gravel and clay–sand–gravel. They visually observed the incipient motion condition in their experimental study and proposed the following relationship

$$(\tau_{cc}/\tau_{cm}) = 0.94(1+P_c)^{3/2}e^{-1/6}(1+0.001UCS^*)^{9/20}, \tag{2}$$

$$UCS^* = UCS/(\rho_S - \rho)gd_a. \tag{3}$$

Here, τ_{cc} is the critical shear stress of cohesive sediment mixture (N/m^2); τ_{cm} the Shields critical shear stress for cohesionless sediment having size equal to arithmetic mean size of cohesive sediment mixture (N/m^2); P_c the clay percentage in fraction by weight; e the void ratio of cohesive sediment mixture; UCS* the dimensionless unconfined compressive strength of cohesive sediment mixture; and UCS is the unconfined compressive strength of cohesive sediment mixture (N/m^2); d_a is arithmetic mean size of the cohesive sediment mixture (m).

The present study exhibits the results of an experimental study on incipient motion of gravel particles in cohesive mixture of clay–silt–gravel and clay–silt–sand–gravel in which clay content varied from 10% to 50%.

Experimental set-up

In the present study, clay, silt, sand and gravel were used as sediments with the median size (d_{50}) of 0.014 mm, 0.062 mm, 0.60 mm and 5.50 mm respectively. The geometric standard deviation for sediment (σ_g) of clay, silt, sand and gravel were 2.06, 1.18, 0.73 and 1.31 respectively. The σ_g was computed as

$$\frac{1}{2}[(d_{84}/d_{50}) + (d_{50}/d_{16})],$$

where d_{84}, d_{50} and d_{16} are the sediment sizes such that 84%, 50% and 16% of the material is finer than the size by dry weight respectively[25].

The experiments were conducted in a tilting flume having 16 m length, 0.75 m width and 0.50 m depth at our laboratory in Roorkee. The channel had a test section of 6 m length, 0.75 m width and 0.18 m depth starting at a distance of 7 m from the channel entrance. The depth of the test section in the channel for sediment filling was 0.18 m. In order to simulate the roughness of the test section on the rest of the flume bed, a thin layer of sediment was pasted uniformly on the rest of the flume bed.

The fresh water (zero salinity) flow in the flume was regulated using a valve provided in the inlet pipe coming from the overhead tank. The discharge was measured volumetrically through a tank provided at the end of the flume.

A rectangular trap, covered with a net-clothing having fine pores, was placed at the end of the flume just after the tail gate. It was used to collect bed load, which was then dried and weighed.

A two-dimensional bed level profiler having least count 1 mm was used to measure the profile of the channel bed. The channel bed profile was also measured by flat gauge of least count 0.10 mm. The water surface profile was measured with a pointer gauge having least count of 0.10 mm. Bed and water surface profile were measured at longitudinal spacing of 0.50 m along the central line of the flume.

Methodology

Two types of cohesive mixtures namely, clay–silt–gravel and clay–silt–sand–gravel were used for preparation of cohesive channel bed in which clay content varied from 10% to 50% on weight basis while the other sediments (i.e. cohesionless sediments) were taken in equal proportions. The dynamic compaction method was used for preparation of the cohesive bed[23]. To prepare the channel bed, the required sediments were dried and weighed as per proportion and then manually mixed together. Water was added to sediment mixture which was then mixed thoroughly. The mixed sediments were covered with polythene and left for around 24 h for uniform moisture distribution. The sediments were mixed thoroughly again before placing into the test section. The sediments were filled in the test section and compacted in three layers for preparing a cohesive bed. Each layer was compacted with a cylindrical roller having a weight equal to 400 N. The sides of channel were compacted by hand rammer having a rectangular bottom. The top surface was roughened by trowel before laying the next layer over it to ensure

Table 1. Range of measured parameters for incipient motion for cohesive mixture in the present study*

Sediment mixture	Number of runs	P_c (%)	d_a (mm)	γ_b (kN/m³)	σ_{cc} (−)	W (%)	UCS (kN/m²)	h (m)	U (m/s)	S_f (−)	R_0 (−)	q_{CI} (N/m-s)	τ_{cc} (N/m²)
Clay–silt–gravel	22	10–50	1.3975–2.5043	16.39–20.60	2.92–5.23	7.72–16.45	0.0–42.17	0.023–0.059	0.306–0.902	0.0045–0.0123	10.21–11.11	0.0010–0.0038	1.301–4.031
Clay–silt–sand–gravel	20	10–50	1.034–1.850	16.96–21.06	4.19–7.49	7.88–18.25	0.0–43.25	0.030–0.066	0.275–0.726	0.0060–0.0165	09.38–10.95	0.0002–0.0013	0.853–2.812

P_c is clay percentage, d_a is arithmetic mean diameter of the cohesive sediment mixture, γ_b is bulk unit weight of the cohesive sediment mixture, σ_{cc} is weighted geometric standard deviation of the cohesive sediment mixture, W is antecedent moisture content of cohesive sediment mixture, UCS is unconfined compressive strength of cohesive sediment mixture, h is average flow depth, U is mean flow velocity, S_f is energy slope, q_{CI} is the transport rate for gravel particles present in the cohesive sediment mixture, τ_{cc} is critical shear stress for the cohesive sediment mixture and Rouse number = $R_0 = w_s/(ku_*)$; where k (von Kármán constant) = 0.41, u_* (shear velocity) = $(\tau_{cc}/\rho)^{1/2}$, ρ is the density of water = 1000 kg/m³, w_s (sediment settling velocity) = $[(Rgd_a^2)/(C_1\upsilon + (0.75C_2Rgd_a^3)^{0.5})]$ is determined as per Ferguson and Church (2004) for sieve diameters for natural grains for which $C_1 = 18.0$ and $C_2 = 1.0$, $R = (\rho_s - \rho)/\rho$, $g = 9.81$ m/s², ρ_s (sediment density) = 2650 kg/m³, υ = kinematic viscosity = 10^{-6} m²/s.

bonding among different layers. Extra sediments were chiselled off using a large sharp edge knife after compacting all three layers. The cohesive bed finally prepared was left for around 16 h to achieve cohesive bonding between the cohesive and non-cohesive matrices. Samples were taken out from the downstream section of cohesive bed for determination of bulk density, unconfined compressive strength and moisture content. The bulk unit weight of sediment mixture was determined using standard core cutter method according to IS-2720 Part XXIX (ref. 26). Unconfined compressive strength (UCS) was determined in the laboratory according to IS-2720 Part X (ref. 27). Water content was determined as per dry oven method for the compacted cohesive bed corresponding to all runs. Dry density of the channel bed was computed using determined value of bulk density and water content of the bed. The void ratio of the channel bed was determined using the computed value of dry density. The range of various parameters related to experimental runs for clay–silt–gravel and clay–silt–sand–gravel mixtures is given in Table 1. Before beginning the experimental run, the bed was saturated for 24 h to achieve the field's condition[23]. For all experimental runs, the sediment beds were prepared afresh.

For each run, a low discharge was initially allowed in the flume and uniform flow was maintained by operating the tail gate. During this process of establishing the uniform flow, the sediment bed was inspected visually to examine the detachment of sediment particles. Then a small increment in the discharge was admitted in the flume and the bed condition was inspected again carefully. This operation was repeated till the movement of gravel particle started. The flow condition at which entrainment of gravel particles occurred was considered as incipient motion condition and measurements of corresponding discharge, water surface profile and bed surface profile were taken. Incipient motion condition for gravel particles present in the cohesive mixture was visually and quantitatively identified by collection of bed load as reported in Table 1. Both water and bed surface profile was meas-

ured at an interval of 0.50 m on the centre line of the test section along the longitudinal direction of flow. The mean velocity was computed using the measured data of discharge and flow depth. Flow depth was computed as an average of difference between the measured bed and water surface profile at the middle of each section at 50 cm interval from upstream working section along the flow direction. The shear stress corresponding to incipient motion of gravel particles was computed using measured flow depth and water surface slope profile. The above process of attaining incipient motion was done for each run.

The physical appearance of the top surface of cohesive bed was observed visually after the end of each run and was found to vary with the clay content in the mixture. After end of incipient motion run, top surface of cohesive bed appeared in the form of sheet and line erosion along with the gravel particles on it for clay content up to 30% for both cohesive mixture of the present study. However, dominancy of gravel particles decreases with increase in clay content in the mixture. The particles eroded in the form of bunch or chunks for 40% and 50% clay content in the mixture and the bed surface appeared like a mass eroded for both cohesive mixtures.

Results and discussion

The critical shear stress for the uniform cohesionless sediment is well represented by the Shields curve, which has also been used in the form of Brownlie[24] equation for computation of dimensionless critical shear stress of the cohesionless sediment[17]. The incipient motion of non-uniform cohesionless sediment is mainly a function of individual sediment size, arithmetic mean size of non-uniform sediment, percentage of sediment and critical shear stress of uniform cohesionless sediment. However in case of cohesive sediment, in addition to the above parameters, clay percentage and strength of cohesive bed play a significant role in entrainment of sediment. The

strength of bed depends on compaction applied on bed and is measured in terms of UCS and reflected by easily measurable parameters such as porosity and bulk density. To incorporate hiding-exposure effect, different forms of correction factors were earlier used to correlate as a function of individual sediment size, arithmetic mean of non-uniform sediment and percentage of sediment. In the present study, hiding-exposure effect was considered in the form of weighted standard deviation of sediment mixture. It is a function of individual sediment size, arithmetic mean size of non-uniform sediment and percentage of sediment. Different forms of correction factors have been tried in trials. However, weighted standard deviation provides the best results and hence used in the present study.

The behaviour of cohesive sediment differs significantly from cohesionless sediment because of the presence of clay in the cohesive sediment mixture. To quantify the effect of cohesion, dimensionless critical shear stress of cohesive sediment mixture (τ_{*cc}) is compared with that of cohesionless sediment having the same arithmetic mean size as that of the cohesive sediment mixture on the plot of Shields parameters as shown in Figure 1 in which abscissa $R_*[=((\rho_s - \rho/\rho)gd_a^3/\upsilon^2)^{0.5}]$ is the dimensionless particle Reynolds number.

Figure 1 shows that the value of τ_{*cc} of gravel particles in a cohesive mixture is higher and much above the line of Shields curve for most data of the present study as well for the data of Kothyari and Jain[13]. However few value of τ_{*cc} lies below the line of Shields curve for the 10–20% of clay content in the mixture. This may be attributed to high silt and low clay content (for 10% and 20% clay content) in the cohesive mixtures of clay–silt–gravel and clay–silt–sand–gravel which led to a weak bond amongst the particles and resulted in exposure of gravel particles at low shear stress.
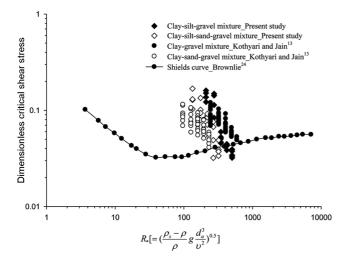

Figure 1. Variation of dimensionless critical shear stress with particle Reynolds number for cohesive sediment mixture and cohesionless sediment.

Development of relationship for critical shear stress

The mechanism of transport of the cohesive sediment including its incipient motion is more complex than the cohesionless sediment. Hence the experiment was performed to account for all aspects. The resistance against erosion of cohesionless sediment was well controlled by the sediment size and density. However, the erosion of cohesive sediment was affected by several parameters due to the complex physico-chemical properties of clay. As such various parameters were considered to develop a relationship for the critical shear stress of gravel particles present in the cohesive sediment mixture. However, only the parameters which yielded better results are represented in the analysis below. Probable variables that affect the critical shear stress of gravel particles present in the cohesive sediment mixtures are written as

$$\tau_{cc} = f(\tau_{cm}, P, P_c, d_{50}, d_a, \sigma_g, \gamma_b, \gamma_w). \tag{4}$$

P is the percentage of individual sediment in the sediment mixture; γ_b the bulk unit weight (N/m^3) of the cohesive sediment mixture and γ_w the unit weight of water (N/m^3). Using dimensional analysis, eq. (4) can be converted into dimensionless form as

$$\frac{\tau_{cc}}{\tau_{cm}} = f\left(P_c, \sigma_{cc}, \frac{\gamma_b}{\gamma_w}\right). \tag{5}$$

Here

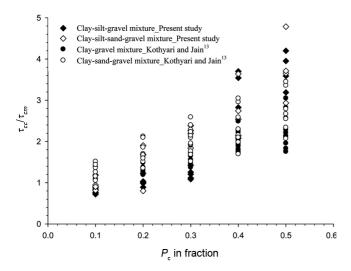$$\sigma_{cc} = \frac{\Sigma(d_{50}.\sigma_g)}{d_a}. \tag{6}$$

σ_{cc} is the weighted geometric standard deviation of the cohesive sediment mixture.

Equation (5) represents the functional relationship corresponding to incipient motion for gravel particles in the cohesive sediment mixtures. Parameter P_c accounts for the presence of clay content in the sediment mixture and the parameter γ_b/γ_w has been considered for the variability of compactness of cohesive bed. The mean size of the cohesive sediment mixture (d_a) is significantly different from the median size (d_{50}) of individual sediments present in the mixture and this variability in sediment sizes creates the hiding-exposure phenomena. Hence to account for this variability, the parameter σ_{cc} has been incorporated. Variation of these parameters, i.e. parameters presented in eq. (5) with τ_{cc}/τ_{cm} is illustrated in Figures 2–4. The value of τ_{cc}/τ_{cm} increases with increase of clay percentage as apparent from Figure 2 for the data of the present study and Kothyari and Jain[13]. Similar results on the variation of clay percentage with the critical
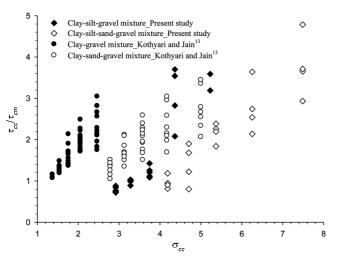
shear stress were reported by Kamphuis and Hall[28]. Figure 3 shows that the value of τ_{cc}/τ_{cm} increases with the increase in σ_{cc} for the data of the present study along with the data of Kothyari and Jain[13]. In earlier studies, the variation of σ_{cc} was not reported. Therefore, the value of σ_{cc} for the data of Kothyari and Jain[13] was computed using eq. (6). Figure 4 indicates that the value of τ_{cc}/τ_{cm} increases with the increase in γ_b/γ_w. Mitchener and Torfs[10] also reported similar results for variation of bulk density against the critical shear stress.
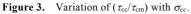
A large number of trials with parameters given in eq. (5) led to the following relationship for the computation of critical shear stress of gravel particles present in cohesive mixture of clay–silt–gravel and clay–silt–sand–gravel

$$\frac{\tau_{cc}}{\tau_{cm}} = 1 + 0.1428 P_c^{1.294} \sigma_{cc}^{0.553} \left(\frac{\gamma_b}{\gamma_w}\right)^{3.814}. \tag{7}$$

The proposed eq. (7) was developed using the data of the present study (clay–silt–gravel and that of clay–silt–sand–gravel mixture) and Kothyari and Jain[13]. The compaction level used in preparation of cohesive channel bed may play a significant role in the entrainment of sediment particles; hence, this compaction level may serve as a limitation of eq. (7) in the present study, which has been reported in Table 2. The computed value of τ_{cc}/τ_{cm} from eq. (7) were plotted against the observed values in Figure 5 which shows good agreement between them as all the data are covered between 0.5 fold and 2.0 fold error lines with a good value of regression coefficient ($R^2 = 0.78$). Here, the present data along with data of Kothyari and Jain[13] have been used. Data of other studies have not been used due to non-availability of critical shear stress data for gravel particles under clay influence.

The mean discrepancy ratio and standard deviation were computed to test the goodness of fit between

Figure 2. Variation of (τ_{cc}/τ_{cm}) with P_c.

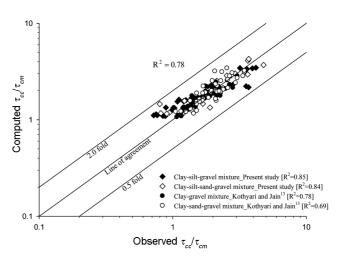**Figure 4.** Variation of (τ_{cc}/τ_{cm}) with (γ_b/γ_w).

Figure 3. Variation of (τ_{cc}/τ_{cm}) with σ_{cc}.

Figure 5. Comparison of observed and computed value of (γ_{cc}/τ_{cm}) using eq. (7).

Table 2. Range of UCS (kN/m^2) for compaction level used in the present study

Cohesive mixture	Sediment proportions (%)				UCS for clay percentage				
					10%	20%	30%	40%	50%
Clay–silt–gravel	Clay	Silt	Sand	Gravel	(0)*	(05.41–07.57)*	(10.27–18.38)*	(18.92–22.17)*	(30.28–42.17)*
	10	45	–	45					
	20	40	–	40					
	30	35	–	35					
	40	30	–	30					
	50	25	–	25					
Clay–silt–sand–gravel	Clay	Silt	Sand	Gravel	(0)*	(06.49–09.73)*	(17.84–20.00)*	(16.76–29.74)*	(19.46–43.25)*
	10	30	30	30					
	20	26.67	26.67	26.67					
	30	23.33	23.33	23.33					
	40	20	20	20					
	50	16.67	16.67	16.67					

*Range of UCS (kN/m^2).

Table 3. Statistical analysis of computed and observed (τ_{cc}/τ_{cm}) as per eqs (8)–(10)*

Equation	Data	Cohesive sediment mixture	N	$\overline{R}$	Discrepancy ratio			σ_{oc}
					% of data in range			
					0.75–1.25	0.75–1.50	0.50–1.50	
Proposed eq. (7)	Present study	Clay–silt–gravel	22	1.175	36	82	91	0.287
		Clay–silt–sand–gravel	20	1.090	70	90	95	0.256
	Kothyari and Jain[13]	Clay–gravel	62	1.020	97	100	100	0.105
		Clay–sand–gravel	46	1.011	89	96	98	0.168
Kothyari and Jain[13] (eq. (2))	Present study	Clay–silt–gravel	22	1.213	27	59	73	0.351
		Clay–silt–sand–gravel	20	1.046	65	85	95	0.291
	Kothyari and Jain[13]	Clay–gravel	62	1.061	100	100	100	0.079
		Clay–sand–gravel	46	0.940	98	98	100	0.122

$\overline{R}$ is mean discrepancy ratio, σ_{oc} is standard deviation for the discrepancy ratio, and N is the total number of observations.

observed and computed value from eq. (7). The following expressions are used for computation of discrepancy ratio, mean discrepancy ratio and standard deviation respectively[29].

$$\text{Discrepancy ratio, } R_i = \frac{(\tau_{cc}/\tau_{cm})_{c,i}}{(\tau_{cc}/\tau_{cm})_{o,i}}. \qquad (8)$$

Here $(\tau_{cc}/\tau_{cm})_{c,i}$ and $(\tau_{cc}/\tau_{cm})_{o,i}$ are the computed and observed value of τ_{cc}/τ_{cm} respectively.

$$\text{The mean discrepancy ratio, } \overline{R} = \frac{\sum_i^N R_i}{N}. \qquad (9)$$

Here, N is the total number of observations.

$$\text{Standard deviation, } \sigma_{oc} = \sqrt{\frac{\sum_i^N (R_i - \overline{R})^2}{N-1}}. \qquad (10)$$

Here σ_{oc} is the standard deviation for the discrepancy ratio.

The proposed eq. (7) and existing eq. (2) are tested against the goodness of fit test using eqs (8)–(10). Table 3 indicates that the proposed eq. (7) shows better results over the existing eq. (2) for critical shear stress of gravel particles in cohesive mixture as more than 80% of data for the present study and Kothyari and Jain[13] lie in the range of 0.75 to 1.50 of discrepancy ratio for the proposed eq. (7). Most importantly, the proposed eq. (7) has the easily computable parameters compared to the existing eq. (2).

Conclusions

This study presents the results of an experimental study on incipient motion of gravel particles in cohesive mixtures of clay–silt–gravel and clay–silt–sand–gravel in which clay content varied from 10% to 50%. The onset of incipient motion, sheet and line erosion pattern occurs on the surface of the bed for clay content up to 30% while the mass erosion pattern occurs for clay content of 40% and 50%. The presence of silt in cohesive mixture

resulted in lowering the value of critical shear stress of gravel particles especially for clay content up to 20% in the cohesive mixture. The present study reveals that initiation of detachment of gravel particles from the cohesive bed is mainly governed by clay percentage, weighted geometric standard deviation and bulk density of cohesive mixture. An equation was proposed for computation of critical shear stress of gravel particle in cohesive mixture. Regression analysis and goodness of fit test indicates that the proposed equation is accurate enough for computation of critical shear stress of gravel particles for the cohesive mixture of clay–gravel, clay–sand–gravel, clay–silt–gravel and clay–silt–sand–gravel.

1. Shields, I. A., Application of similarity principles and turbulence research to bed-load movement. Publication No. 167, California Institute of Technology, Pasadena, 1936, pp. 1–36.
2. Iwagaki, Y., Hydrodynamical study on critical tractive force. *Trans. JSCE*, 1956, 41, 1–21.
3. Yang, C. T., Incipient motion and sediment transport. *J. Hydraul. Div.*, 1973, **99**, 1679–1704.
4. Yalin, M. S. and Karahan, E., Inception of sediment transport. *J. Hydraul. Div.*, 1979, **105**, 1433.
5. Singh, M., Singh, I. B. and Müller, G., Sediment characteristics and transportation dynamics of the Ganga River. *Geomorphology*, 2007, **86**, 144–175.
6. Arora, C., Bhaskaran, Jain, P. K., Bhar, I., Bhar, A. and Narayana, A. C., Bottom boundary layer characteristics in the Hooghly estuary under combined wave-current action. *Mar. Geod.*, 2010, **33**, 261–281.
7. Arora, C. and Bhaskaran, P. K., Parameterization of bottom friction under combined wave-tide action in the Hooghly estuary, India. *Ocean Eng.*, 2012, **43**, 43–55.
8. Arora, C. and Bhaskaran, P. K., Numerical modeling of suspended sediment concentration and its validation for the Hooghly estuary, India. *Coast. Eng. J.*, 2013, **55**, 1–23.
9. Arora, C., Bhaskaran, P. K., and Narayana, A. C., Influence of particle shape on drag coefficient for commonly occurring sandy particles in coastal areas. *Int. J. Ocean Clim. Syst.*, 2010, **1**, 99–112.
10. Mitchener, H. and Torfs, H., Erosion of mud/sand mixtures. *Coast. Eng.*, 1996, **29**(1–2), 1–25.
11. Ansari, S. A., Kothyari, U. C. and Ranga Raju, K. G., Incipient motion characteristics of cohesive sediments. *ISH J. Hydraul. Eng.*, 2007, **13**, 108–121.
12. Ahmad, M. F., Dong, P., Mamat, M., Nik, W. B. W. and Mohd, M. H., The critical shear stresses for sand and mud mixture. *Appl. Math. Sci.*, 2011, **5**, 53–71.
13. Kothyari, U. C. and Jain, R. K., Influence of cohesion on the incipient motion condition of sediment mixtures. *Water Resour. Res.*, 2008, **44**, 1–15.
14. Kuhnle, R. A., Incipient motion of sand-gravel sediment mixtures. *J. Hydraul. Eng.*, 1993, **119**, 1400–1415.
15. Patel, P. L. and Ranga Raju, K. G., Fractionwise calculation of bed load transport. *J. Hydraul. Res.*, 1996, **34**, 363–379.
16. Wu, W., Wang, S. S. Y. and Jia, Y., Nonuniform sediment transport in alluvial rivers. *J. Hydraul. Res.*, 2000, **38**, 427–434.
17. Dong, P., Two-fraction formulation of critical shear stresses for sand and silt mixtures. *J. Waterw. Port, Coastal, Ocean Eng.*, 2007, **133**, 238–241.
18. Bridge, J. S. and Bennett, S. J., A model for the entrainment and transport of sediment grains of mixed sizes, shapes, and densities. *Water Resour. Res.*, 1992, **28**, 337–363.
19. Sutarto, T., Papanicolaou, A. N., Wilson, C. G. and Langendoen, E. J., Stability analysis of semicohesive streambanks with CONCEPTS: Coupling field and laboratory investigations to quantify the onset of fluvial erosion and mass failure. *J. Hydraul. Eng.*, 2014, **140**, 1–19.
20. Einstein, H. A., Formulas for the transportation of bed load. *Trans. Am. Soc. Civ. Eng.*, 1942, **107**, 561–577.
21. Meyer-Peter, E. and Müller, R., Formulas for bed-load transport. In Proceedings of the 2nd Meeting of the International Association of Hydraulic Research, IAHR, 1948, pp. 39–64.
22. Misri, R. L., Garde, R. J. and Ranga Raju, K. G., Bed load transport of coarse nonuniform sediment. *J. Hydraul. Eng.*, 1984, **110**, 312–328.
23. Jain, R. K., Influence of cohesion on detachment and transport of clay-sand-gravel mixtures. Ph.D. Thesis, Department of Civil Engineering, Indian Institute of Technology Roorkee, Roorkee, India, 2008.
24. Brownlie, W. R., Prediction of flow depth and sediment discharge in open channels. Report No. KH-R-43A, W. M. Keck Laboratory of Hydraulics and Water Resources, California Institute of Technology, Pasadena, California, 1981, pp. 1–232.
25. Garde, R. J. and Ranga Raju, K. G., Mechanics of sediment transportation and alluvial stream problems. 3rd edn., New Age International, New Delhi, 2000, pp. 1–712.
26. IS (Bureau of Indian Standards), Determination of in-place density by core-cutter method. IS-2720, Part XXIX, New Delhi, 1975, pp. 1–9.
27. IS (Bureau of Indian Standards), Determination of shear strength by unconfined compression method. IS-2720, Part X, New Delhi, 1991, pp. 1–4.
28. Kamphuis, J. W. and Hall, K. R., Cohesive material erosion by unidirectional current. *J. Hydraul. Eng.*, 1983, **109**, 49–61.
29. Yang, C. T., Molinas, A. and Wu, B., Sediment transport in the Yellow River. *J. Hydraul. Eng.*, 1996, **122**, 237–244.